




# Solution-processed mixed halide $\text{CH}_3\text{NH}_3\text{PbI}_{3-x}\text{Cl}_x$ thin films prepared by repeated dip coating

A. M. M. Tanveer Karim<sup>1</sup>, M. S. Hossain<sup>1</sup>, M. K. R. Khan<sup>2,\*</sup> , M. Kamruzzaman<sup>3</sup>, M. Azizar Rahman<sup>4</sup>, and M. Mozibur Rahman<sup>2</sup>

<sup>1</sup>Department of Physics, Rajshahi University of Engineering & Technology, Rajshahi 6204, Bangladesh

<sup>2</sup>Department of Physics, University of Rajshahi, Rajshahi 6205, Bangladesh

<sup>3</sup>Department of Physics, Begum Rokeya University, Rangpur 5400, Bangladesh

<sup>4</sup>Department of Physics, Bangladesh University of Engineering and Technology, Dhaka 1000, Bangladesh

Received: 6 March 2019

Accepted: 1 June 2019

Published online:  
11 June 2019

© Springer Science+Business  
Media, LLC, part of Springer  
Nature 2019

## ABSTRACT

The mixed halide  $\text{CH}_3\text{NH}_3\text{PbI}_{3-x}\text{Cl}_x$  crystalline thin film has been prepared by two-step solution-processed repeated dip coating method at an ambient atmosphere. X-ray diffraction study reveals the presence of tetragonal and cubic phases in deposited film. Raman study confirms the metal halide bond in the inorganic framework and organic  $\text{CH}_3$  stretching/bending of C–H bond in  $\text{CH}_3\text{NH}_3\text{PbI}_{3-x}\text{Cl}_x$  perovskite. Scanning electron microscopy shows that cuboid and polyhedral-like crystal grains of 100 nm to 2  $\mu\text{m}$  may find applications in optoelectronics. The perovskite  $\text{CH}_3\text{NH}_3\text{PbI}_{3-x}\text{Cl}_x$  thin film shows high spectral absorption coefficient of the order of  $10^6 \text{ m}^{-1}$ . In optical band gap study, we found the coexistence of cubic and tetragonal perovskite phases. The energy band gap is dominated by cubic phase having  $E_g = 2.50 \text{ eV}$  over tetragonal phase with band gap  $E_g = 1.67 \text{ eV}$ . The room-temperature photoluminescence study confirms band edge, shallow and deep-level emissions. The temperature-dependent cathodoluminescence study shows red, green and ultraviolet emissions. The dominating green luminescence evolved for cubic phase at 2.51 eV. The red and ultraviolet emissions are also found for mixed-phase  $\text{CH}_3\text{NH}_3\text{PbI}_{3-x}\text{Cl}_x$  thin film, suitable for preparation of light-emitting devices.

## Introduction

The ability of solution-processed organic–inorganic perovskites  $\text{CH}_3\text{NH}_3\text{PbX}_3$  ( $X = \text{Br}, \text{I}$  and  $\text{Cl}$ ) to convert visible light into electricity was first discovered in 2006 using  $\text{CH}_3\text{NH}_3\text{PbBr}_3$  as a sensitizer on nanoporous  $\text{TiO}_2$  in a liquid electrolyte-based dye-

sensitized solar cells, but the device power conversion efficiency (PCE) was found low [1]. Researchers try to boost up the PCE of solar cells using perovskite nanoparticles or thin film over conventional dyes replacing the halogen site partially but PCE still unsatisfactory. At room temperature, methyl ammonium lead tri-iodide ( $\text{CH}_3\text{NH}_3\text{PbI}_3$ ) forms a

Address correspondence to E-mail: fkrkhan@yahoo.co.uk

tetragonal structure of band gap  $\sim 1.5$ – $1.7$  eV, whereas  $\text{CH}_3\text{NH}_3\text{PbBr}_3$  and  $\text{CH}_3\text{NH}_3\text{PbCl}_3$  form cubic structure of band gap  $\sim 1.5$ – $2.30$  eV and  $\sim 3.0$ – $3.11$  eV, respectively [2, 3]. Among these perovskites,  $\text{CH}_3\text{NH}_3\text{PbI}_3$  and  $\text{CH}_3\text{NH}_3\text{PbBr}_3$  are immensely used in photovoltaic and optoelectronic applications. In comparison with these perovskites,  $\text{CH}_3\text{NH}_3\text{PbCl}_3$  remains overlooked to scientific community and have not investigated extensively.  $\text{CH}_3\text{NH}_3\text{PbCl}_3$  is a wide band gap material which exhibits high optical absorption coefficient in the UV spectral range [3]. Therefore,  $\text{CH}_3\text{NH}_3\text{PbCl}_3$  can be used as a visible-blind UV photodetector and hole transport layer for highly efficient organic light-emitting diodes [3, 4]. Researchers are trying to tune the band gap of perovskites in between 1.5 and 3.11 eV to generate a significant advancement for photovoltaic's and light-emission applications. The band gap of perovskites can be tuned by different approaches. Inclusion of organic or inorganic cations can alter the band gap of perovskites [5]. Partial substitution of halogen anions such as Cl at iodide site can convert the parent halide perovskite to mixed halide perovskite ( $\text{CH}_3\text{NH}_3\text{PbI}_{3-x}\text{Cl}_x$ ) and tune the band gap of parent halide perovskites. It can also modify the physical properties of parent perovskites [6, 7]. At room temperature,  $\text{CH}_3\text{NH}_3\text{PbI}_{3-x}\text{Cl}_x$  contains tetragonal crystal structure similar to  $\text{CH}_3\text{NH}_3\text{PbI}_3$  but exhibits exceptional optoelectronic properties, such as tunable direct band gap ranging from UV to near-IR [8], strong light absorption, high photoluminescence quantum efficiency, high charge-carrier mobility, low recombination rates etc. [9, 10]. Recently, the solar power conversion efficiency of mixed halide perovskite has been reported to 23.7% [11]. Apart from this, mixed halide perovskites are intensively investigated for light emitters in LED's and lasers [12]. Despite progress has been achieved in terms of preparation and conversion efficiency of mixed halide perovskites, still some issues such as the presence of Cl by part at I or Br sites and its effect on structural and physical properties of  $\text{CH}_3\text{NH}_3\text{PbI}_{3-x}\text{Cl}_x$  remain still important in correlation with preparation condition and technique. Furthermore, it has been reported that thin-film growth parameters and post-treatment process such as ultrasonic substrate vibration [13, 14] and short-time annealing [15–17] can also play an important role for the modification of structural, morphological, tuning of band gap and luminescence properties of perovskite thin films.

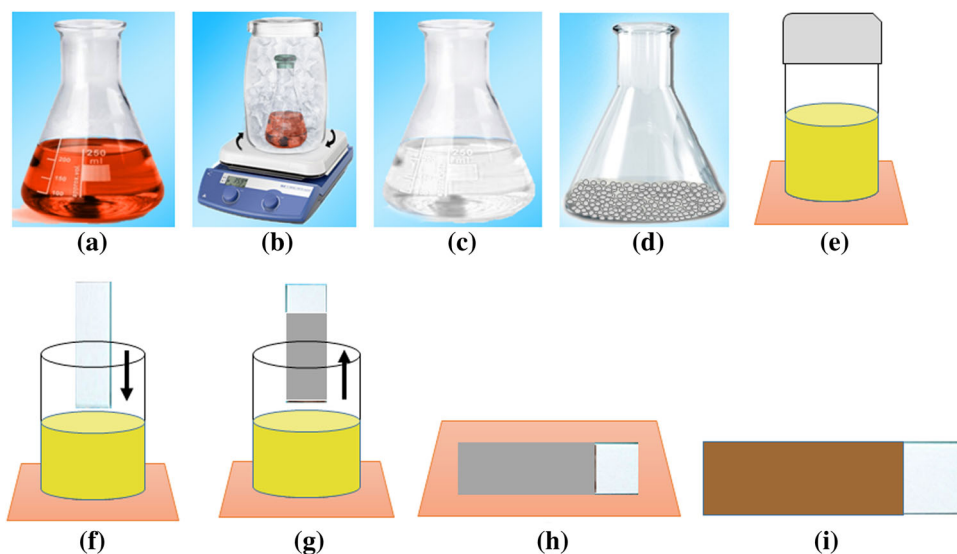
Several physical and chemical deposition techniques including some new solution-processed casting methods, such as doctor blading, inkjet printing, screen printing, drop casting, slot-die coating, roll-to-roll printing, etc. [18, 19], have been employed to fabricate high-quality  $\text{CH}_3\text{NH}_3\text{PbI}_{3-x}\text{Cl}_x$  thin films. However, all these methods are a bit more expensive due to use of vacuum environment and also cause difficulties in controlling film compositions. In most cases, the precursor solution of mixed halide perovskite was prepared in a globe box at nitrogen atmosphere with a rotary evaporator which is expensive and complex process. However, in this work our main focus concentrates on cost-effective production of chlorinated perovskite film by repeated dip coating technique at air ambient and studies the effects of the partial replacement of I by Cl on structural, optical and electronic properties in order to understand photovoltaic and optoelectronic applications.

Previously, we reported multi-color emissions of  $\text{CH}_3\text{NH}_3\text{PbI}_{3-x}\text{Cl}_x$  thin film prepared by chemical dip-coating technique at ambient atmosphere [20]. In this paper, we show the coexistence of tetragonal and cubic phases in  $\text{CH}_3\text{NH}_3\text{PbI}_{3-x}\text{Cl}_x$  thin film deposited on glass substrate by repeated dip coating method at ambient atmosphere. The grown film is capable of showing high absorption coefficient, tuning the traditional band gap of perovskite and displaying strong colored emission peaks at 2.51 eV (green luminescence). The reason for the coexistence of cubic and tetragonal phases and their role on physical properties have been explained on the basis of the result of the X-ray diffraction (XRD), scanning electron microscope (SEM), Raman spectroscopy, ultraviolet (UV)-visible spectroscopy, photoluminescence (PL) and temperature-dependent cathodoluminescence (CL) experiments.

## Experimental section

Preparation of perovskite solution and deposition of  $\text{CH}_3\text{NH}_3\text{PbI}_{3-x}\text{Cl}_x$  thin film by repeated dip coating technique is performed in an ambient atmosphere illustrated in Fig. 1. The details of the preparation of perovskite solutions are described in our previous work [20]. For the preparation of chlorinated perovskite film, prepared solution was heated at  $(80 \pm 10)$  °C for 30 min and then a clean glass

**Figure 1** Schematics for preparation of perovskite solution and dip coating technique for the synthesis of  $\text{CH}_3\text{NH}_3\text{PbI}_{3-x}\text{Cl}_x$  thin film.



substrate was dipped into the solution for 10 s and then taken out from glass container (g) dried in air for 05 s. This process of dip coating cycle was performed for four to five times to complete the film growth process. The ash (h) color of pristine film changed from ash to dark brown (i) when heated on a hot plate at 100 °C for 5 min. Similar changes of color after heating were reported by [21, 22].

X-ray diffraction (XRD) data of prepared sample were collected from a BRUKER D8 advance X-ray diffractometer in between Bragg angle of (10–50)° with  $\text{CuK}_\alpha$  radiation of wavelength  $\lambda = 0.154$  nm. The surface morphology of the film was studied by a ZEISS EVO 18 Research scanning electron microscope (SEM). The phonon vibrational modes of the film were recorded by Renishaw in via Raman spectrometer using 514.5 nm line of  $\text{Ar}^+$  ion laser. Optical transmission and reflection were recorded using UV-1601PC SHIJMADZU spectrophotometer. Room-temperature photoluminescence (RTPL) measurement was performed using an F-4600, Hitachi spectrofluorophotometer at an excitation wavelength,  $\lambda_{\text{ex}} = 500$  nm. Cathodoluminescence (CL) spectra were recorded at temperatures 80 K and 300 K using FEI Quanta 200 ESEM connected to ocean optics spectrometer. The thickness of the deposited film was measured using Newton's rings method [23–25] at the middle of the film area (1 cm × 1 cm). The film thickness was found out from the difference between the diameter of the rings of the interference pattern formed on the film surface and glass substrate using the relation,

$$t = \frac{r_n^2 - r'_n{}^2}{2R} \quad (1)$$

where  $r_n$  is the radius of the ring with film,  $r'_n$  is the radius of the ring without film,  $R$  is the radius of curvature of plano-convex lens used and  $t$  is the film thickness. The experiment was performed for 4 to 5 times at different places in the film area (1 cm × 1 cm) and the average film thickness was estimated to ~ 160 nm.

## Results and discussion

### Structural analysis

Figure 2 shows the XRD pattern of mixed halide perovskite thin film. The presence of diffraction peaks at Bragg angles  $2\theta \approx 15.55^\circ$ ,  $22.11^\circ$ ,  $35.22^\circ$  and  $38.88^\circ$  is corresponding to (1 0 0), (1 1 0), (2 1 0) and (2 1 1) reflections of the cubic (\*) trichloride ( $\text{CH}_3\text{NH}_3\text{PbCl}_3$ ) phase [26]. The remaining reflection peaks at (1 1 0), (2 2 0), (3 1 0) and (2 2 4) corresponding to angles  $14.20^\circ$ ,  $28.55^\circ$ ,  $31.77^\circ$  and  $40.55^\circ$  are representing the tetragonal (#)  $\text{CH}_3\text{NH}_3\text{PbI}_{3-x}\text{Cl}_x$  phase [27, 28]. A very low intensity peak at around  $12.77^\circ$  corresponding to (0 0 1) plane corresponds to  $\text{PbI}_2$  (■) phase due to decomposition of  $\text{CH}_3\text{NH}_3\text{PbI}_{3-x}\text{Cl}_x$  in the air [27]. It is reported that cubic phase of  $\text{CH}_3\text{NH}_3\text{PbCl}_3$  is transformed into tetragonal phase when synthesized below 54 °C, whereas tetragonal to cubic phase transformation occurred when annealed at 100 °C [29]. In this work, we have prepared

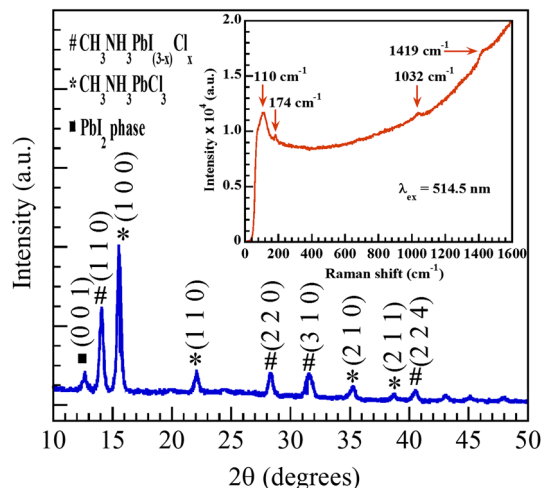


**Figure 2** XRD pattern of dipping-deposited  $\text{CH}_3\text{NH}_3\text{PbI}_{3-x}\text{Cl}_x$  thin film shows the presence of cubic (\*), tetragonal (#) and  $\text{PbI}_2$  (■) phases. Inset shows the vibrational Raman spectrum excited at  $\lambda_{\text{ex}} = 514.5$  nm.

$\text{CH}_3\text{NH}_3\text{PbI}_{3-x}\text{Cl}_x$  film at  $80^\circ\text{C}$  and annealed at  $100^\circ\text{C}$  in air ambient. From XRD pattern of annealed film (Fig. 2), it is clear that there are two major intensity peaks, one corresponding to (1 0 0) plane which is a signature of cubic  $\text{CH}_3\text{NH}_3\text{PbCl}_3$  phase; while other corresponding to (1 1 0) plane denotes the tetragonal  $\text{CH}_3\text{NH}_3\text{PbI}_{3-x}\text{Cl}_x$  phase. This XRD result is suggesting that cubic and tetragonal phases can coexist for the film annealed at  $100^\circ\text{C}$ . Similar coexistence of cubic and tetragonal phases was reported by Luo et al. [29] for spin-coated  $\text{CH}_3\text{NH}_3\text{PbI}_3$  film which converted to  $\text{CH}_3\text{NH}_3\text{PbCl}_3$  when annealed at  $100^\circ\text{C}$  for 10 min and further annealing at the same temperature for 45 min,  $\text{CH}_3\text{NH}_3\text{PbCl}_3$  again converted to an intermediate phase to  $\text{CH}_3\text{NH}_3\text{PbI}_3$  due to template effect. In general, it is established that cubic  $\text{CH}_3\text{NH}_3\text{PbCl}_3$  phase is originated by placing of methylammonium ( $\text{MA}^+$ ) cations forming  $\text{C}_{3v}$  molecular symmetry in between the cavities of a three-dimensional array of  $\text{PbCl}_6$  octahedra. The  $\text{MA}^+$  cations perform complex rotation and orientation to satisfy the site symmetry occupying  $\text{O}_h$  sites, whereas Pb atom occupies three chlorine atoms that lie on  $\text{D}_{4h}$  sites [30, 31] in one of each per unit cell. However, large ionic difference of  $\text{Cl}^-$  and  $\text{I}^-$  ions makes the formation energy for  $\text{CH}_3\text{NH}_3\text{PbI}_{3-x}\text{Cl}_x$  higher compared to cubic  $\text{CH}_3\text{NH}_3\text{PbCl}_3$  phase and helps to dominant  $\text{CH}_3\text{NH}_3\text{PbCl}_3$  over  $\text{CH}_3\text{NH}_3\text{PbI}_{3-x}\text{Cl}_x$  phase. Therefore, the structural modulation of perovskite  $\text{CH}_3\text{NH}_3\text{PbI}_3$  replacing I by Cl may

induce the variation of electronic and optical properties which may create avenue to cater photovoltaic and optoelectronic applications [32].

### Raman spectroscopy analysis

The vibrational mode of deposited  $\text{CH}_3\text{NH}_3\text{PbI}_{3-x}\text{Cl}_x$  film has been investigated by means of vibrational Raman spectroscopy in the range of  $100\text{--}1600\text{ cm}^{-1}$ , as shown in inset of Fig. 2. From this figure, it is seen that there are four distinct vibrational modes centered at  $110$ ,  $174$ ,  $1032$  and  $1419\text{ cm}^{-1}$ , respectively. The vibrational modes centered at  $110$  and  $174\text{ cm}^{-1}$  are for tetragonal  $\text{CH}_3\text{NH}_3\text{PbI}_{3-x}\text{Cl}_x$  [33] phase corresponding to the hetero-polar ionic/covalent interactions of metal and halide bond (Pb–X bond) in the inorganic framework [34]. On the other hand, the vibrational mode of cubic  $\text{CH}_3\text{NH}_3\text{PbCl}_3$  phase is found at  $1419\text{ cm}^{-1}$  corresponding to  $\text{CH}_3$  stretching [35] or C–H bending [36] bonds. Furthermore, the vibrational mode for organic part ( $\text{CH}_3\text{N H}_3^+$ ) is found at  $1032\text{ cm}^{-1}$  [37]. It is noted that the coexistence of cubic and tetragonal phases is evidenced by Raman spectroscopy as well.

### Surface morphology

Surface morphology of solution-processed mixed halide perovskite plays a vital role in optoelectronic applications. The topology of scanning electron microscope (SEM) image of  $\text{CH}_3\text{NH}_3\text{PbI}_{3-x}\text{Cl}_x$  perovskite is shown in inset of Fig. 3. The SEM image indicates that film is composed of cuboids and polyhedral-like shapes with grain sizes  $100\text{ nm}$  to  $2\text{ }\mu\text{m}$  consistent to [38, 39] distributed all over the film surface. Such large grain size perovskites are suitable for efficient charge transfer, reduction in exciton recombination and making high-performance optoelectronic devices [40]. It is also reported that spin-coated large grain size films by ultrasonic vibration improves device performances [7].

To confirm the presence of Cl in the deposited film, elemental analysis was done by energy-dispersive X-ray spectroscopy (EDS) for uncoated  $\text{CH}_3\text{NH}_3\text{PbI}_{3-x}\text{Cl}_x$  sample as shown in Fig. 3. The EDS spectrum shows peaks for C, O, Si, Na and Cl atoms using K-series X-rays and Pb atoms for M-series X-rays, respectively. The presence of O, Si and Na peaks in the spectrum originated from soda lime glass substrate. It is important to note that the EDS spectrum



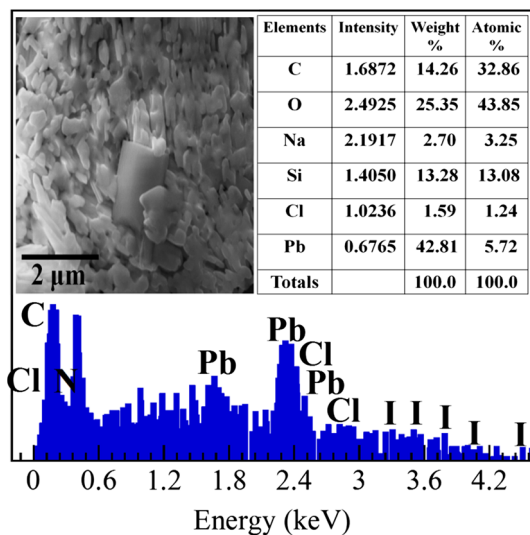


**Figure 3** EDS analysis of deposited  $\text{CH}_3\text{NH}_3\text{PbI}_{3-x}\text{Cl}_x$  thin film. The corresponding SEM image (inset) showing the large cuboid and polyhedral crystals.

reveals the presence of Cl in the deposited film. The atomic % of the different elements present in the film is shown in table (inset) of Fig. 3.

### Optical studies

The absorption coefficient ( $\alpha$ ) was calculated from transmission  $T(\lambda)$  and reflection  $R(\lambda)$  data using the relation [41–44]

$$\alpha = \frac{1}{t} \ln \left[ \frac{[1 - R(\lambda)]^2}{T(\lambda)} \right] \quad (2)$$

where  $t$  is film thickness. The variation of  $\alpha$  with photon energy for the  $\text{CH}_3\text{NH}_3\text{PbI}_{3-x}\text{Cl}_x$  thin film is shown in the inset of Fig. 4. The film displays high absorption coefficient of the order of  $10^6 \text{ m}^{-1}$  in both visible and near-IR spectral ranges. The large value of  $\alpha$  seems to arise from s–p antibonding coupling of mixed halide perovskite [45]. It is noted that the absorption coefficient is minimum at wavelength  $\sim 740 \text{ nm}$  which corresponds to traditional band gap 1.67 eV for tetragonal phase of  $\text{CH}_3\text{NH}_3\text{PbI}_{3-x}\text{Cl}_x$ . However, the sharp band edge wavelength at around 500 nm is corresponding to the band gap energy 2.50 eV of mixed-phase perovskite.

The optical band gap ( $E_g$ ) of the mixed halide perovskite film for direct transition can be expressed by the following equation [46]

$$(\alpha h\nu)^2 = A(h\nu - E_g) \quad (3)$$

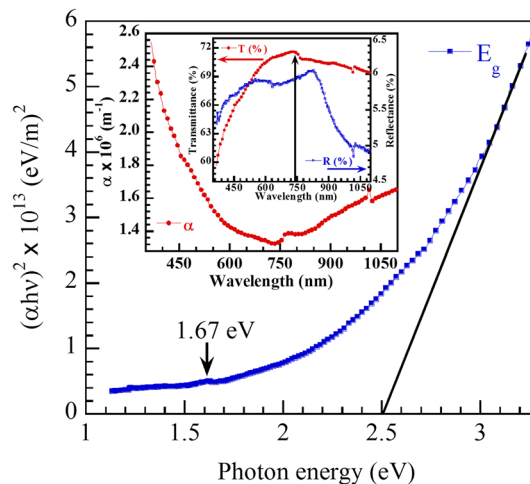


**Figure 4** Plot of  $(\alpha h\nu)^2$  vs photon energy for direct transition in dipping-deposited  $\text{CH}_3\text{NH}_3\text{PbI}_{3-x}\text{Cl}_x$  thin film. In inset, the variation of the absorption coefficient, the optical transmittance (left scale) and reflectance (right scale) spectra with wavelength of dipping-deposited  $\text{CH}_3\text{NH}_3\text{PbI}_{3-x}\text{Cl}_x$  thin film.

where  $A$  is the band edge constant related to the effective masses associated with the valence and conduction bands and  $h\nu$  is the photon energy. The value of the optical band gap for the absorption could be estimated by extrapolating the linear portion of Eq. (2), and the intercept of the energy axis of Fig. 4 gives the value of  $E_g$ . The estimated band gap is found to be 2.50 eV which is lower than 3.0 eV for cubic  $\text{CH}_3\text{NH}_3\text{PbCl}_3$  phase but higher than 1.6 eV for traditional  $\text{CH}_3\text{NH}_3\text{PbI}_{3-x}\text{Cl}_x$  phase [1, 27, 28]. Thus, the tuning of the band gap mainly results from the interaction of cubic and tetragonal phases in which cubic phase is dominant over tetragonal phase for which we got  $E_g = 2.50 \text{ eV}$  for cubic phase. This value is close to the band gap  $E_g = 3.0 \text{ eV}$  of cubic perovskite. Our XRD experiment also demonstrated higher volume of cubic phase over tetragonal phase. This effect lowers the recombination process because of the replacement of excess halogen ions in heavy metal element Pb with organic framework. It is also noted that some relativistic effects such as spin–orbit coupling and higher electronegativity between the metal cation and halide anion may increase the band gap of  $\text{CH}_3\text{NH}_3\text{PbI}_{3-x}\text{Cl}_x$  film. A small peak at  $\sim 1.67 \text{ eV}$  is also observed in Fig. 4 (shown by an arrow) which may arise due to the optical transitions of the free carriers for the tetragonal phase of the deposited perovskite.

## Photoluminescence study

Photoluminescence (PL) is one of the useful techniques to characterize the optical properties of semi-conducting materials. The room-temperature PL measurement of the  $\text{CH}_3\text{NH}_3\text{PbI}_{3-x}\text{Cl}_x$  thin film was performed at an excitation wavelength,  $\lambda_{\text{ex}} = 500$  nm, as shown in Fig. 5.

In the spectrum, a very intense luminescence peak at 1.64 eV and two weak peaks at 2.01 eV and 2.11 eV are observed. The optical band gap estimated by optical transmittance measurement is tuned to 2.5 eV, which suggests the presence of both  $\text{CH}_3\text{NH}_3\text{PbI}_{3-x}\text{Cl}_x$  and  $\text{CH}_3\text{NH}_3\text{PbCl}_3$  phases. Therefore, PL emission at 1.64 eV may be due to band edge (BE) emission which attributed to the free carriers' exciton. Besides, BE emission at 1.64 eV, two other emissions at 2.01 eV and 2.11 eV refer to either of the shallow-level defects of vacancies or interstitials of organic part, otherwise deep-level defects of halogen interstitials or anti-sites of lead and halogen as suggested by DFT calculations [47]. These defects states are related to the preparation method which allows a particular chemical structure with Cl-containing polycrystalline system having higher polarization along the C–N...Cl axis [31].

## Temperature-dependent cathodoluminescence study

The cathodoluminescence (CL) is an advanced technique that detects simultaneously secondary

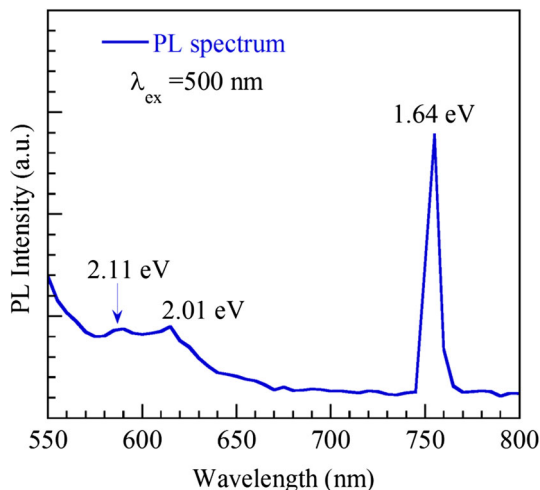


**Figure 5** RTPL spectrum of dipping-deposited  $\text{CH}_3\text{NH}_3\text{PbI}_{3-x}\text{Cl}_x$  film excited at  $\lambda_{\text{ex}} = 500$  nm.

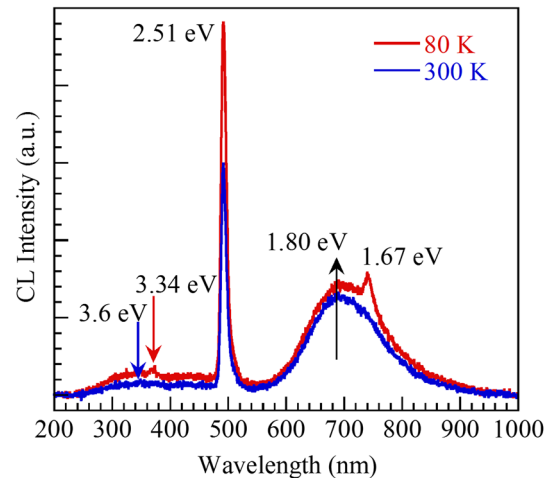


**Figure 6** Cathodoluminescence spectra of dipping-deposited  $\text{CH}_3\text{NH}_3\text{PbI}_{3-x}\text{Cl}_x$  thin film at temperatures 80 K and 300 K.

electrons and light emissions which correlate the physical structure of the material to its local transport and optical properties of the sample. The CL measurement of  $\text{CH}_3\text{NH}_3\text{PbI}_{3-x}\text{Cl}_x$  thin film was carried out at 10 nA electron beam current with an accelerating voltage of 10 kV at temperatures 80 K and 300 K as shown in Fig. 6.

In the cathodoluminescence spectrum, a sharp emission of green luminescence (GL) peak at 2.51 eV is in between the band gap energies for tetragonal (1.6 eV) and cubic (3.0 eV) phases suggesting the interaction of tetragonal  $\text{CH}_3\text{NH}_3\text{PbI}_{3-x}\text{Cl}_x$  and cubic  $\text{CH}_3\text{NH}_3\text{PbCl}_3$  phases. There are few other broader emission peaks found at 1.67 eV and 1.80 eV corresponding to red luminescence (RL) and very weak peaks at 3.34 eV and 3.60 eV for ultraviolet luminescence (UVL), respectively. It should be noted that the emissions at 3.34 eV and 3.6 eV are the frequency doubling of emissions at 1.67 eV and 1.80 eV, respectively, known as harmonic emissions. However, the CL peak intensity is found lower for 300 K than the intensity at 80 K. This lowering of intensity is the direct evidence of decreasing recombination events with increasing temperature [48].

## Conclusions

In summary,  $\text{CH}_3\text{NH}_3\text{PbI}_{3-x}\text{Cl}_x$  thin film has been successfully prepared by repeated dip coating method at an ambient atmosphere. Structural results provide an evidence of the formation of both tetragonal  $\text{CH}_3\text{NH}_3\text{PbI}_{3-x}\text{Cl}_x$  and cubic  $\text{CH}_3\text{NH}_3\text{PbCl}_3$

phases in the deposited film. Raman study confirms the metal halide bond in the inorganic framework and organic CH<sub>3</sub> stretching/bending of C–H bond in CH<sub>3</sub>NH<sub>3</sub>PbI<sub>3-x</sub>Cl<sub>x</sub> perovskite. From SEM image, it is clear that the film surface is compact and composed of cuboids and polyhedral grains having high absorption coefficient of the order of 10<sup>6</sup> m<sup>-1</sup> in both visible and near-IR spectral regions. Photoluminescence study confirms band edge accompanied with shallow and deep-level defect emissions. The green luminescence at 2.51 eV from cathodoluminescence study confirms the interaction between tetragonal CH<sub>3</sub>NH<sub>3</sub>PbI<sub>3-x</sub>Cl<sub>x</sub> and cubic CH<sub>3</sub>NH<sub>3</sub>PbCl<sub>3</sub> phases. Importantly, this work presents an easy and effective method for the deposition of CH<sub>3</sub>NH<sub>3</sub>PbI<sub>3-x</sub>Cl<sub>x</sub> thin film with large grain size useful for high-performance perovskite optoelectronic devices.

## Acknowledgements

Authors are thankful to the department of Glass and Ceramic Engineering, Rajshahi University of Engineering & Technology, Bangladesh, for providing XRD and SEM facilities. The authors are also grateful to the Department of Materials Science and Engineering, City University of Hong Kong, for providing Raman spectroscopy measurement. One of the authors M. Azizar Rahman acknowledges the financial support of Australian Government through the Research Training Program Scholarship.

## References

- [1] Chen Q, De Marco N, Yang Y, Song TB, Chen CC, Zhao H, Hong Z, Zhou H, Yang Y (2015) Under the spotlight: the organic-inorganic hybrid halide perovskite for optoelectronic applications. *Nano Today* 10:355–396
- [2] Huang J, Xiang S, Yu J, Li C-Z (2019) Highly efficient prismatic perovskite solar cells. *Energy Environ Sci* 12:1265–1273
- [3] Nandi P, Giri C, Swain D, Manju U, Topwal D (2019) Room temperature growth of CH<sub>3</sub>NH<sub>3</sub>PbCl<sub>3</sub> single crystals by solvent evaporation method. *CrystEngComm* 21:656–661
- [4] Zheng E, Yuh B, Tosado GA, Yu Q (2017) Solution-processed visible-blind UV-A photodetectors based on CH<sub>3</sub>NH<sub>3</sub>PbCl<sub>3</sub> perovskite thin films. *J Mater Chem C* 5:3796–3806
- [5] Pang G, Lan X, Li R, He Z, Chen R (2019) Influence of mixed organic cations on the structural and optical properties of lead tri-iodide perovskites. *Nanoscale* 11:5215–5221
- [6] Ansari MIH, Qurashi A, Nazeeruddin MK (2018) Frontiers, opportunities and challenges in perovskite solar cells: a critical review. *J Photochem Photobiol C* 35:1–24
- [7] Xionga H, Zabiha F, Wanga H, Zhanga Q, Eslamian M (2018) Grain engineering by ultrasonic substrate vibration post treatment of wet perovskite films for annealing-free, high performance, and stable perovskite solar cells. *Nanoscale* 10:8526–8535
- [8] Yakunin S, Shynkarenko Y, Dirin DN, Cherniukh I, Kovalenko MV (2017) Non-dissipative internal optical filtering with solution-grown perovskite single crystals for full-colour imaging. *NPG Asia Mater* 9:e431
- [9] Chin S-H, Choi JW, Woo HC, Kim JH, Lee HS, Lee C-L (2019) Realizing a highly luminescent perovskite thin film by controlling the grain size and crystallinity through solvent vapour annealing. *Nanoscale* 11:5861–5867
- [10] Kim H, Zhao L, Price JS, Grede AJ, Roh K, Brigeman AN, Lopez M, Rand BP, Giebink NC (2018) Hybrid perovskite light emitting diodes under intense electrical excitation. *Nat Commun* 9:4893
- [11] <http://www.nrel.gov/pv/assets/images/efficiency-chart.png>. Accessed 23 Dec 2018
- [12] Stranks SD, Hoyer RLZ, Di D, Friend RH, Deschler F (2018) The physics of light emission in halide perovskite devices. *Adv Mater*. <https://doi.org/10.1002/adma.201803336>
- [13] Ahmadian-Yazdi M-R, Habibi M, Eslamian M (2018) Excitation of wet perovskite films by ultrasonic vibration improves the device performance. *Appl Sci* 8:308
- [14] Ahmadian-Yazdi M-R, Eslamian M (2018) Toward scale-up of perovskite solar cells: annealing-free perovskite layer by low-cost ultrasonic substrate vibration of wet films. *Mater Today Commun* 14:151–159
- [15] Lee JW, Yu H, Lee K, Bae S, Kim J, Han GR, Hwang D, Kim SK, Jang J (2019) Highly crystalline perovskite-based photovoltaics via two-dimensional liquid cage annealing strategy. *J Am Chem Soc* 141:5808–5814
- [16] Lee B, Hwang T, Lee S, Shin B, Park B (2019) Microstructural evolution of hybrid perovskites promoted by chlorine and its impact on the performance of solar cell. *Sci Rep* 9:4803
- [17] Sanches AWP, da Silva MAT, Cordeiro NJA, Urbano A, Lourenço SA (2019) Effect of intermediate phases on the optical properties of PbI<sub>2</sub>-rich CH<sub>3</sub>NH<sub>3</sub>PbI<sub>3</sub> organic-inorganic hybrid perovskite. *Phys Chem Chem Phys* 21:5253–5261

- [18] Wang Q, Phung N, Girolamo DD, Vivo P, Abate A (2019) Enhancement in lifespan of halide perovskite solar cells. *Energy Environ Sci* 12:865–886
- [19] Habibi M, Rahimzadeh A, Bennouna I, Eslamian M (2017) Defect-free large-area (25 cm<sup>2</sup>) light absorbing perovskite thin films made by spray coating. *Coatings* 7:42
- [20] Karim AMMT, Rahman MA, Hossain MS, Khan MKR, Rahman MM, Kamruzzaman M, Ton-That C (2018) Multi-color excitonic emissions in chemical dip-coated organolead mixed-halide perovskite. *Chem Sel* 3:6525–6530
- [21] Adnan M, Lee JK (2018) All sequential dip-coating processed perovskite layers from an aqueous lead precursor for high efficiency perovskite solar cells. *Sci Rep* 8:2168
- [22] Chen J, Wan Z, Liu J, Fu S-Q, Zhang F, Yang S, Tao S, Wang M, Chen C (2018) Growth of compact CH<sub>3</sub>NH<sub>3</sub>PbI<sub>3</sub> thin films governed by the crystallization in PbI<sub>2</sub> matrix for efficient planar perovskite solar cells. *ACS Appl Mater Interfaces* 10:8649–8658
- [23] Wahl KJ, Chromik RR, Lee GY (2008) Quantitative in situ measurement of transfer film thickness by a Newton's rings method. *Wear* 264:731–736
- [24] Winston AW, Baer CA, Allen LR (2013) A simple film thickness gauge utilizing Newton's rings. In: *Proceedings of the sixth national symposium on vacuum technology transactions*, pp 249–254
- [25] Raveesha KH, Doddamani VH, Prasad BK (2014) On a method to employ Newton's rings concept to determine thickness of thin films. *Int Lett Chem Phys Astron* 22:1–7
- [26] Maculan G, Sheikh AD, Abdelhady AL, Saidaminov MI, Haque MA, Murali B, Alarousu E, Mohammed OF, Wu T, Bakr OM (2015) CH<sub>3</sub>NH<sub>3</sub>PbCl<sub>3</sub> Single crystals: inverse temperature crystallization and visible-blind UV-photodetector. *J Phys Chem Lett* 6:3781–3786
- [27] Yu H, Wang F, Xie F, Li W, Chen J, Zhao N (2014) The role of chlorine in the formation process of "CH<sub>3</sub>NH<sub>3</sub>PbI<sub>3-x</sub>Cl<sub>x</sub>" perovskite. *Adv Funct Mater* 24:7102–7108
- [28] Xu Y, Zhu L, Shi J, Lv S, Xu X, Xiao J, Dong J, Wu H, Luo Y, Li D, Meng Q (2015) Efficient hybrid mesoscopic solar cells with morphology-controlled CH<sub>3</sub>NH<sub>3</sub>PbI<sub>3-x</sub>Cl<sub>x</sub> derived from two-step spin coating method. *ACS Appl Mater Interfaces* 7:2242–2248
- [29] Luo S, Daoud WA (2016) Crystal structure formation of CH<sub>3</sub>NH<sub>3</sub>PbI<sub>3-x</sub>Cl<sub>x</sub> perovskite. *Materials* 9:123
- [30] Chi L, Swainson I, Cranswicka L, Her JH, Stephens P, Knop O (2005) The ordered phase of methylammonium lead chloride CH<sub>3</sub>ND<sub>3</sub>PbCl<sub>3</sub>. *J Solid State Chem* 178:1376–1385
- [31] Dimesso L, Dimamay M, Hamburger M, Jaegermann W (2014) Properties of CH<sub>3</sub>NH<sub>3</sub>PbX<sub>3</sub> (X = I, Br, Cl) powders as precursors for organic/inorganic solar cells. *Chem Mater* 26:6762–6770
- [32] Sedighi R, Tajabadi F, Shahbazi S, Gholipour S, Taghavinia N (2016) Mixed-halide CH<sub>3</sub>NH<sub>3</sub>PbI<sub>3-x</sub>X<sub>x</sub> (X = Cl, Br, I) perovskites: vapor-assisted solution deposition and application as solar cell absorbers. *Chem Phys Chem* 17:2382–2388
- [33] Pistor P, Ruiz A, Cabot A, Roca VI (2016) Advanced Raman spectroscopy of methylammonium lead iodide: development of a non-destructive characterisation methodology. *Sci Rep* 6:35973
- [34] Niemann RG, Kontos AG, Palles D, Kamitsos EI, Kaltzoglou A, Brivio F, Falaras P, Cameron PJ (2016) Halogen effects on ordering and bonding of CH<sub>3</sub>NH<sub>3</sub><sup>+</sup> in CH<sub>3</sub>NH<sub>3</sub>PbX<sub>3</sub> (X = Cl, Br, I) hybrid perovskites: a vibrational spectroscopic study. *J Phys Chem C* 120:2509–2519
- [35] Maalej A, Abid Y, Kallel A, Daoud A, Lauti A, Romain F (1997) Phase transitions and crystal dynamics in the cubic perovskite CH<sub>3</sub>NH<sub>3</sub>PbCl<sub>3</sub>. *Solid State Commun* 103:279–284
- [36] Brivio F, Frost JM, Skelton JM, Jackson AJ, Weber OJ, Weller MT, Goni AR, Leguy AMA, Barnes PRF, Walsh A (2015) Lattice dynamics and vibrational spectra of the orthorhombic, tetragonal, and cubic phases of methylammonium lead iodide. *Phys Rev B* 92:144308
- [37] Glaser T, Muller C, Sendner M, Krekeler C, Semonin OE, Hull TD, Yaffe O, Owen JS, Kowalsky W, Pucci A, Lovrincic R (2015) Infrared spectroscopic study of vibrational modes in methylammonium lead halide perovskites. *J Phys Chem Lett* 6:2913–2918
- [38] Dong Q, Yuan Y, Shao Y, Fang Y, Wang Q, Huang J (2015) Abnormal crystal growth in CH<sub>3</sub>NH<sub>3</sub>PbI<sub>3-x</sub>Cl<sub>x</sub> using a multi-cycle solution coating process. *Energy Environ Sci* 8:2464–2470
- [39] Xiao L, Xu J, Luan J, Yu X, Zhang B, Dai S, Yao J (2018) Preparation of CH<sub>3</sub>NH<sub>3</sub>PbCl<sub>3</sub> film with a large grain size using PbI<sub>2</sub> as Pb source and its application in photodetector. *Mater Lett* 220:108–111
- [40] Gedamu D, Asuo IM, Benetti D, Basti M, Ka I, Cloutier SG, Rosei F, Nechache R (2018) Solvent-antisolvent ambient processed large grain size perovskite thin films for high-performance solar cells. *Sci Rep* 8:12885
- [41] Moss TS (1959) *Optical properties of semiconductor*. Academic Press, New York
- [42] Karim AMMT, Khan MKR, Rahman MM (2015) Structural and opto-electrical properties of pyrolyzed ZnO–CdO crystalline thin films. *J Semicond* 36:053001
- [43] Ashaduzzman M, Khan MKR, Karim AMMT, Rahman MM (2018) Influence of chromium on structural, non-linear optical constants and transport properties of CdO thin films. *Surf Interfaces* 12:135–144
- [44] Islam MA, Karim AMMT, Julkarnain M, Badrul AKM, Khan MKR, Khan KA (2017) Opto-transport properties of



- e-beam evaporated annealed CuInSe<sub>2</sub> thin films. *Surf Interfaces* 8:170–175
- [45] Song TB, Chen Q, Zhou H, Jiang C, Wang HH, Yang YM, Liu Y, Youab J, Yang Y (2015) Perovskite solar cells: film formation and properties. *J Mater Chem A* 3:9032–9050
- [46] Tauc J (1974) *Amorphous and liquid semiconductors*. Plenum Press, New York
- [47] Buin A, Pietsch P, Voznyy O, Comin R, Ip AH, Sargent EH, Xu B (2014) Materials processing routes to trap-free halide perovskites. *Nano Lett* 14:6281–6286
- [48] Jiang DS, Jung H, Ploog K (1988) Temperature dependence of photoluminescence from GaAs single and multiple quantum-well heterostructures grown by molecular-beam epitaxy. *J Appl Phys* 64:1371

**Publisher's Note** Springer Nature remains neutral with regard to jurisdictional claims in published maps and institutional affiliations.